JP Journal of Heat and Mass Transfer
© 2025 Pushpa Publishing House, Prayagraj, India
https://pphmjopenaccess.com
https://doi.org/10.17654/0973576325042 P-ISSN: 0973-5763
Volume 38, Number 6, December 2025, Pages 795-809 E-ISSN: 3049-2556

RESPONSE SURFACE ANALYSIS (RSA) OF CARBON NANOTUBES-WATER FLOW IN A POROUS MEDIUM

Najiyah Safwa Khashi'ie[1,*], Mohd Fariduddin Mukhtar[2], Mohd Fadzli Bin Abdollah[1], Abdul Rahman Mohd Kasim[3] and Mikhail Sheremet[4]

[1]Fakulti Teknologi dan Kejuruteraan Mekanikal
Universiti Teknikal Malaysia Melaka
76100 Durian Tunggal, Melaka, Malaysia
e-mail: najiyah@utem.edu.my

[2]Fakulti Pengurusan Teknologi Dan Teknousahawanan
Universiti Teknikal Malaysia Melaka
76100 Durian Tunggal, Melaka, Malaysia

[3]Pusat Sains Matematik
Universiti Malaysia Pahang Al-Sultan Abdullah
Lebuh Persiaran Tun Khalil Yaakob
26300 Pahang, Malaysia

Received: August 8, 2025; Revised: October 25, 2025; Accepted: October 29, 2025

Keywords and phrases: convective flow, Darcy model, single nanofluid, porous medium, response surface analysis, optimization.

*Corresponding author

How to cite this article: Najiyah Safwa Khashi'ie, Mohd Fariduddin Mukhtar, Mohd Fadzli Bin Abdollah, Abdul Rahman Mohd Kasim and Mikhail Sheremet, Response surface analysis (RSA) of carbon nanotubes-water flow in a porous medium, JP Journal of Heat and Mass Transfer 38(6) (2025), 795-809. https://doi.org/10.17654/0973576325042

Published Online: December 11, 2025

[4]Laboratory on Convective Heat and Mass Transfer
Tomsk State University
36 Lenin Avenue, 634050 Tomsk, Russia

Abstract

This work investigates the thermal behavior of single-walled carbon nanotube (SWCNT) nanofluid flow over a stretchable plate embedded in a porous medium using the Darcy-Forchheimer-Brinkman formulation. The study is motivated by the growing demand for efficient heat transfer enhancement in porous-based thermal systems and advanced cooling technologies. A combined numerical-statistical framework is developed, integrating the local non-similarity (LNS) method with response surface methodology (RSM) to identify and optimize key factors influencing the heat transfer rate. The novelty lies in coupling RSM with the Darcy-Forchheimer-Brinkman model for CNT-based nanofluid flow, providing a new pathway to predict and optimize thermal performance. The analysis reveals that the Darcy number exerts the greatest influence on heat transfer, whereas magnetic and nanoparticle parameters contribute minimally. The study recommends extending this approach to hybrid or tetra nanofluids to achieve superior performance in porous media cooling and energy applications.

Nomenclature

B_0	Strength (constant) of the magnetic field
Da	Darcy number
g	Gravitational acceleration
F_c	Forchheimer coefficient
k_{pm}	Thermal conductivity ($Wm^{-1}K^{-1}$)
K	Permeability of the porous media
M	Magnetic parameter

Ri	Richardson number
T	Temperature (K)
u, v	velocity in the x-, y-directions, respectively (ms^{-1})
x, y	Cartesian coordinates (m)
α	Inclined magnetic field's angle (in degree)
ε	Porosity of the Alumina ceramic
γ	Darcy permeability parameter

1. Introduction

Nanofluid flow through a porous media has been an area of significant research interest due to its applications in thermal management, cooling systems and energy devices. For instance, Hussain and Sheremet [1] analyzed the convection of radiative nanofluid flow in porous media with inclined magnetic fields, providing valuable insights into the thermal behavior of nanofluids under the influence of external magnetic fields. Khashi'ie et al. [2] explored the magnetohydrodynamic (MHD) stagnation point flow over a shrinking/stretching surface in a porous medium, focusing on double stratification effects. Recent work by Alao et al. [3] focused on viscous heating and thermal gyration of magneto-micropolar fluid particles in a porous fixed channel with internal non-uniform heat generation, addressing the combined effects of magnetic fields and internal heat generation. Recent papers on this topic involving various types of fluids can be found in references [4-8].

Many researchers have opted numerical techniques, statistical data analysis and optimization in examining the boundary layer flow including the changes in input parameters which affect the flow behavior and solution. Numerical analysis involves developing and applying computational methods to solve the governing boundary layer model, while the statistical data analysis identifies which factors most strongly influence the boundary layer characteristics. Khashi'ie et al. [9] found that the suction parameter has higher sensitivity to the heat transfer (more dominant) than the heat generation and magnetic parameters. Meanwhile, Venkatadri et al. [10] analyzed the non-Darcy flow in TiO_2/Cu-water hybrid nanofluid subjected to a differentially heated square enclosure using Lattice Boltzmann Method and RSM with sensitivity analysis. Further, both RSM and sensitive analysis were also used by Panda et al. [11] in the optimization of the heat transfer rate. Other papers which reported and utilized statistical data analysis as well as the optimization and sensitivity analysis can be found in these references [12-14].

The choice of the numerical approach in this research is motivated by its ability to accurately solve complex partial differential equations (PDEs) that describe nanofluid flow in porous media. The Darcy-Forchheimer-Brinkman model has been widely recognized for modelling fluid flow in porous media, taking into account the effects of both porosity and permeability. Numerical methods have been successfully applied in various studies to analyze boundary layer flow and heat transfer in nanofluid systems. However, most of these studies have either focused solely on numerical solutions or have limited the scope of their analyses to specific parameter ranges without incorporating a broader statistical analysis to understand the sensitivity of their findings.

Despite numerous studies on nanofluid flow and heat transfer in porous media, limited attention has been given to integrating statistical optimization techniques with detailed numerical modelling for single-walled carbon nanotube (SWCNT) nanofluids under the Darcy-Forchheimer-Brinkman framework. Previous research has primarily emphasized either purely numerical approaches or restricted parameter analyses without exploring the combined influence of multiple governing factors on the overall thermal performance. In this study, a novel hybrid framework combining the local non-similarity (LNS) method and the response surface methodology (RSM) is developed to perform both numerical and sensitivity analyses. This integration enables the identification of the most dominant parameters influencing heat transfer while providing an optimized prediction model for

CNT-based nanofluid flow in porous media. Hence, the main novelty of this work lies in the coupled use of RSM with the Darcy-Forchheimer-Brinkman model for SWCNT-water nanofluid, offering a new perspective on the optimization of heat transfer performance in porous thermal systems.

2. Mathematical Formulation

The nanofluid flow (SWCNTs-H_2O) is assumed to move over a stretching sheet saturated in a porous medium (alumina ceramic) with velocity $U_w(x) = cx.$ Based on main reference [1], the governing model is

$$\frac{\partial u}{\partial x} + \frac{\partial v}{\partial y} = 0, \tag{1}$$

$$\frac{1}{\varepsilon^2}\left(u\frac{\partial u}{\partial x} + v\frac{\partial u}{\partial y}\right) = \nu_{nf}\left(\frac{1}{\varepsilon}\frac{\partial^2 u}{\partial y^2} - \frac{u}{K}\right) - \frac{F_c}{\sqrt{K}}u^2$$

$$+ g\frac{(\rho\beta)_{nf}}{\rho_{nf}}(T - T_\infty) - \frac{\sigma_{nf}}{\rho_{nf}}\sin^2\alpha B_0^2 u, \tag{2}$$

$$u\frac{\partial T}{\partial x} + v\frac{\partial T}{\partial y} = \frac{k_{eff}}{(\rho C_p)_{nf}}\frac{\partial^2 T}{\partial y^2} + \frac{\varepsilon\mu_{nf}}{(\rho C_p)_{nf}}\frac{u^2}{K}, \tag{3}$$

$$\left.\begin{array}{l} u = U_w(x),\ v = 0,\ T = T_w \text{ at } y = 0 \\ u \to 0,\ T \to T_\infty \text{ as } y \to \infty \end{array}\right\}, \tag{4}$$

and

$$k_{eff} = (1 - \varepsilon)k_{pm} + \varepsilon k_{nf}.$$

where

$$F_c = \frac{1.75}{\sqrt{150\varepsilon^3}}$$

is the Forchheimer coefficient, k_{pm} stands for the porous material's thermal conductivity. This transformation is used to simplify the model

$$\eta = y\sqrt{\frac{c}{\nu_f}}, \quad \xi = \frac{x}{l}, \quad \theta(\xi, \eta) = \frac{T - T_\infty}{T_w - T_\infty},$$

$$u = cx\frac{\partial f}{\partial \eta}, \quad v = -\sqrt{c\nu_f}\left(f + \xi\frac{\partial f}{\partial \xi}\right). \tag{5}$$

Equations (2)-(4) are now reduced to:

$$\frac{\partial^3 f}{\partial \eta^3} = \frac{C_1}{\varepsilon}\left[\left(\frac{\partial f}{\partial \eta}\right)^2 - f\frac{\partial^2 f}{\partial \eta^2} + \xi\left(\frac{\partial f}{\partial \eta}\frac{\partial^2 f}{\partial \xi \partial \eta} - \frac{\partial^2 f}{\partial \eta^2}\frac{\partial f}{\partial \xi}\right)\right] + \varepsilon\gamma\frac{\partial f}{\partial \eta}$$

$$+ \varepsilon\left[\frac{C_1 F_c}{Da}\xi\left(\frac{\partial f}{\partial \eta}\right)^2 + C_2\frac{\partial f}{\partial \eta}M\sin^2\alpha - C_3 Ri\xi^{-1}\theta\right], \tag{6}$$

$$\frac{C_4}{Pr}\frac{\partial^2 \theta}{\partial \eta^2} = \xi\left(\frac{\partial f}{\partial \eta}\frac{\partial \theta}{\partial \xi} - \frac{\partial \theta}{\partial \eta}\frac{\partial f}{\partial \xi}\right) - C_5\varepsilon\gamma\xi^2 Ec\left(\frac{\partial f}{\partial \eta}\right)^2 - f\frac{\partial \theta}{\partial \eta}, \tag{7}$$

$$\frac{\partial f}{\partial \eta}(\xi, 0) = 1,\ \xi\frac{\partial f}{\partial \xi}(\xi, 0) + f(\xi, 0) = 0,\ \theta(\xi, 0) = 1,$$

$$\frac{\partial f}{\partial \eta}(\xi, \eta) \to 0, \quad \theta(\xi, \eta) \to 0 \text{ as } \eta \to \infty, \tag{8}$$

where

$$C_1 = \frac{\rho_{nf}/\rho_f}{\mu_{nf}/\mu_f},\ C_2 = \frac{\sigma_{nf}/\sigma_f}{\mu_{nf}/\mu_f},\ C_3 = \frac{(\rho\beta)_{nf}/(\rho\beta)_f}{\mu_{nf}/\mu_f},$$

$$C_4 = \frac{k_{eff}/k_f}{(\rho C_p)_{nf}/(\rho C_p)_f} \text{ and } C_5 = \frac{\mu_{nf}/\mu_f}{(\rho C_p)_{nf}/(\rho C_p)_f}.$$

Meanwhile, the parameters used are as follows:

(a) $M = \sigma_f B_0^2/c\rho_f$ - magnetic parameter,

(b) $\gamma = \nu/cK$ - Darcy permeability parameter,

(c) $Da = \sqrt{K}/l$ - Darcy number, and

(d) $Ri = g\beta_f(T_w - T_\infty)/lc^2$ - Richardson number.

The correlations of nanofluid and the specific properties of the nanoparticles can be found in Hussain and Sheremet [1]. The equations represent skin friction and thermal rate are (see Hussain and Sheremet [1]):

$$Re^{1/2}C_f = \frac{\mu_{nf}}{\mu_f}\xi^{-1}\left(\frac{\partial^2 f}{\partial\eta^2}\right)_{\eta=0}, \quad Re^{-1/2}Nu = -\xi\frac{k_{eff}}{k_f}\left(\frac{\partial\theta}{\partial\eta}\right)_{\eta=0}. \tag{9}$$

3. Local Non-similarity (LNS) Method

The similarity transformation is widely regarded as the most common approach for nondimensionalizing the governing equations of boundary layer flow. Nevertheless, its effectiveness diminishes in certain physical scenarios, as it fails to significantly reduce the number of governing variables. To overcome this limitation, the method of local non-similarity (LNS) is employed. By introducing a set of reasonable assumptions, this approach yields a system of ordinary differential equations (ODEs) corresponding to each level of truncation. Due to the intricate structure of equations (6)-(8), obtaining exact analytical solutions is unfeasible, thus necessitating the application of the LNS method at its first level of truncation. In this level, the expressions consisting of $\xi\partial(\ )/\partial\xi$ are assumed to be very small and omitted. The first truncation level refers to the equations (6)-(8):

$$f''' = \frac{C_1[f'^2 - f f'']}{\varepsilon} + \varepsilon\gamma f'$$

$$+ \varepsilon\left[\frac{C_1 F_c \xi f'^2}{Da} + C_2 M f' \sin^2\alpha - C_3 Ri\xi^{-1}\theta\right], \tag{10}$$

$$\frac{C_4}{Pr}\theta'' = -f\theta' - C_5\varepsilon\gamma\xi^2 Ec f'^2, \tag{11}$$

$$f' = 1,\ f = 0,\ \theta = 1,\ \text{at}\ \eta = 0,$$

$$f' \to 0,\ \theta \to 0\ \text{as}\ \eta \to \infty. \tag{12}$$

For the second truncation level, refers to the equations (10)-(12):

$$\frac{\partial f}{\partial \xi} = h, \quad \frac{\partial \theta}{\partial \xi} = g, \quad \frac{\partial h}{\partial \xi} = \frac{\partial g}{\partial \xi} = 0. \tag{13}$$

Therefore, for the second truncation level, the transformed equations are

$$h''' = \frac{C_1}{\varepsilon}[3h'f' - 2hf'' - fh'' + \xi(h')^2 - \xi hh''] + \varepsilon\gamma h' + C_2\varepsilon Mh'\sin^2\alpha$$
$$+ \varepsilon\left[\frac{C_1 F_c}{Da}(2\xi h'f' + f'^2) - C_3 Ri(\xi^{-1}g - \xi^{-2}\theta)\right], \tag{14}$$

$$\frac{C_4}{Pr}g'' = \xi(gh' - hg') + f'g - fg' - h\theta' - \theta' h$$
$$- C_5\varepsilon Ec\gamma(2\xi^2 h'f' + 2\xi f'^2), \tag{15}$$

$$g = 0, \quad h' = 0, \quad h = 0, \text{ at } \eta = 0,$$
$$g \to 0, \quad h' \to 0, \text{ as } \eta \to \infty. \tag{16}$$

4. Results and Discussion

The bvp4c function (Matlab) is used to compute the equations in the previous section. The range of the magnetic parameter was chosen to explore the effects of varying magnetic field strengths on the thermal behaviour, which is critical in applications such as electromagnetic casting, metalworking, and MHD-based cooling technologies. The Darcy number range was selected to simulate different porosity levels of the porous medium, aligning with natural geological formations and engineered porous materials like alumina ceramic used in insulation or filtration systems. The nanoparticle concentration range for single-walled carbon nanotubes (SWCNTs) was chosen based on their established thermal conductivity enhancement properties in nanofluids. Additionally, the selected values allow for a detailed sensitivity analysis to reveal the most influential factors in the optimization of heat transfer, which was a key focus of this study. Table 1 presents the validation of the numerical results. In this study, the benchmark cases were established based on previously validated results by Hussain and Sheremet [1] and benchmarked against their numerical results for the limiting case as stated in Table 1. The computed skin friction coefficient values in the current work matched closely with those reported by Hussain and Sheremet [1]. This benchmarking ensures that the proposed numerical procedure (LNS-bvp4c solver) reproduces known solutions accurately before extending to the full parametric study. Therefore, the inclusion of these reference cases provides a standardized and validated foundation that enhances the robustness, accuracy and credibility of the present results.

Table 1. Model validation of $-f''(0)$ when $\alpha = 90^\circ$, $\phi = \gamma = Ri = Ec = 0$, $\varepsilon = \xi = 1$ and $Da \to \infty$

M	Present	Hussain and Sheremet [1]
0.5	1.7321	1.7320
1.0	1.5811	1.5811
1.5	1.4142	1.4142
2.0	1.2247	1.2247

Meanwhile, magnetic, Darcy number and nanoparticles' concentration are varied for three testing values (low, medium and high magnitudes) while other parameters are fixed; $Ec = 0$, $\gamma = 0.7$, $Ri = 5$ and $\alpha = 60^\circ$. The RSM is important in the identification of the factor settings which optimize the response including to develop a model for the curvature in the data. The sensitivity of the results to the chosen physical parameters was thoroughly analyzed using RSM, which enabled a detailed examination of how variations in key factors affect the heat transfer performance. The data collection in this study is based on the computational simulation of the nanofluid flow over a stretchable plate in a porous medium using the Darcy-Forchheimer-Brinkman model. A central composite design (CCD) was employed, which provided 20 simulation runs at different levels of the parameters to ensure a robust and comprehensive analysis. These runs were then analyzed statistically to determine the sensitivity of the heat transfer coefficient to each parameter. In Table 2, the response surface design from Minitab software which employs the central composite design with 3 factors and 20 runs is highlighted.

Table 2. Experimental design with RSM

Run	Real parameters			
	M	Da	ϕ	Coefficient of heat transfer
1	1.5	0.01	0	2.8257
2	1.5	0.03	0.02	3.1466
3	0.5	0.02	0.01	3.2042
4	0.5	0.03	0.01	3.2921
5	1.5	0.01	0.02	2.8087
6	0.5	0.02	0.01	3.2042
7	0	0.01	0.02	2.8842
8	0	0.02	0.01	3.2408
9	0.5	0.02	0.01	3.2042
10	0.5	0.02	0.02	3.1418
11	0	0.03	0	3.4015
12	0.5	0.02	0.01	3.2042
13	0.5	0.02	0.01	3.2042
14	1.5	0.02	0.01	3.0312
15	0	0.01	0	2.9000
16	0.5	0.01	0.01	2.8203
17	0.5	0.02	0	3.1604
18	0.5	0.02	0.01	3.2042
19	0	0.03	0.02	3.2674
20	1.5	0.03	0	3.2763

The sensitivity function given in equation (18) is derived from the response function in equation (17),

$$y = 3.1854 - 0.0605A + 0.2145B - 0.0315C - 0.0213A^{*}A - 0.1011B^{*}B - 0.0062C^{*}C - 0.0120AB + 0.0004AC - 0.0289BC, \quad (17)$$

$$\frac{\partial y}{\partial A} = -0.0605 - 0.0426A - 0.0120B + 0.0004C,$$

$$\frac{\partial y}{\partial B} = 0.2145 - 0.2022B - 0.0120A - 0.0289C,$$

$$\frac{\partial y}{\partial C} = -0.0315 - 0.0124C + 0.0004A - 0.0289B. \quad (18)$$

Figure 1 presents the sensitivity analysis for variables *A*, *B* and *C* in relation to heat transfer. The lengths of the bars serve as visual indicators, with longer bars reflecting greater sensitivity and shorter bars indicating lesser sensitivity. Darcy number (B) has the most pronounced impact on heat transfer, showing greater sensitivity as compared to variables *A* and *C*. Additionally, the negative sensitivity values for magnetic (A) and nanoparticle concentrations (C) imply an inverse relationship, indicating that a decrease in these variables would correspond to an increase in heat transfer. Specifically, increasing the magnetic field strength did not lead to significant improvements in heat transfer, while higher concentrations of nanoparticles sometimes resulted in diminishing returns due to the potential for increased fluid viscosity or particle aggregation. This finding is consistent with previous studies [1], where porous medium permeability has been identified as a critical factor in controlling fluid flow and heat transfer in nanofluid systems.

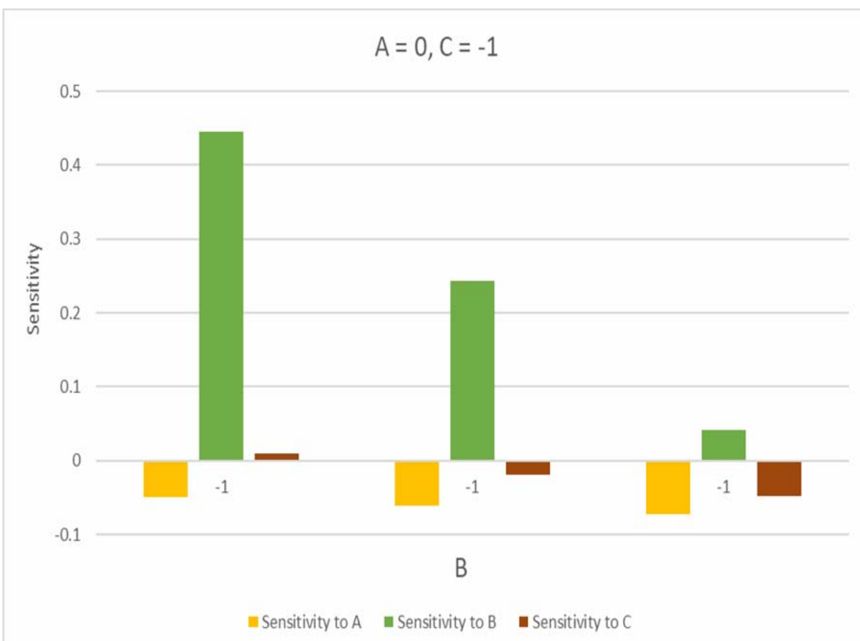

(a)

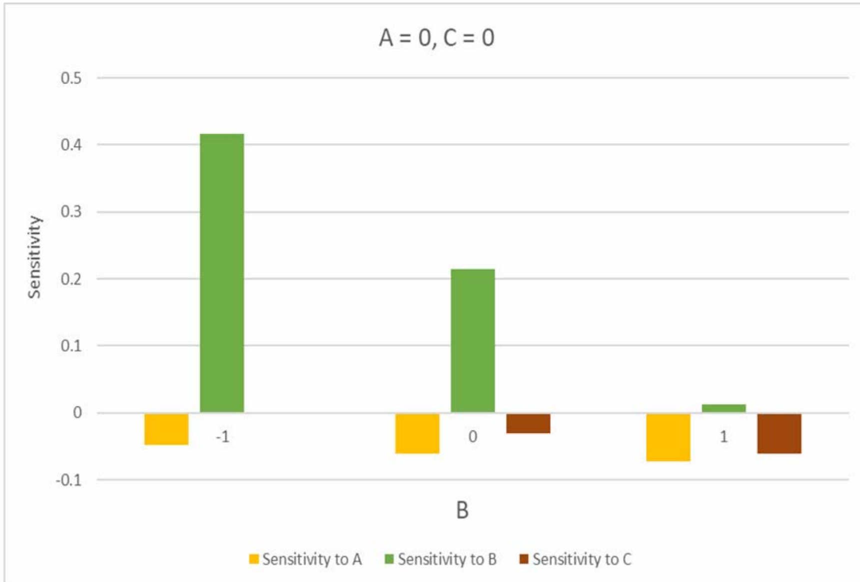

(b)

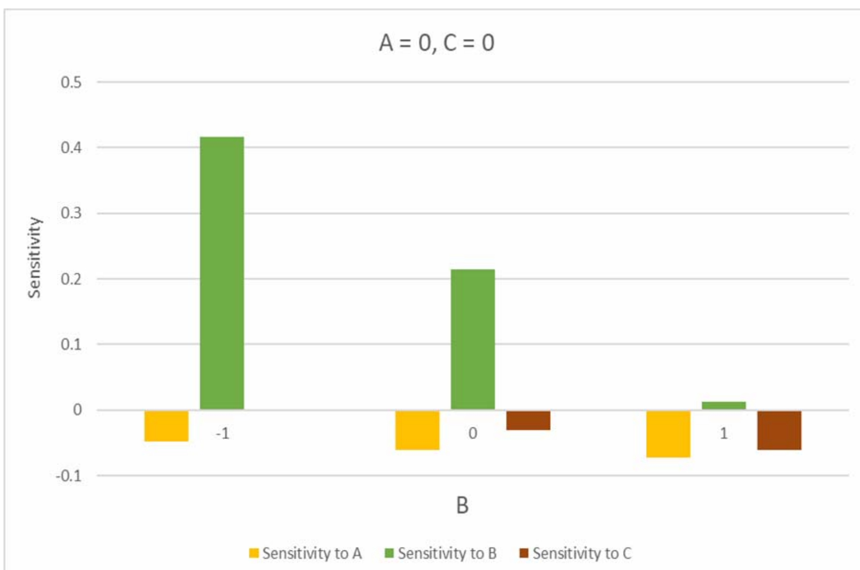

(c)

Figure 1. Sensitivity analysis for each variable for (a) $A = 0,\ C = -1,$ (b) $A = 0,\ C = 0$ and (c) $A = 0,\ C = 1.$

5. Conclusions

This study focused on the numerical and response surface analysis of nanofluid flow over a stretchable plate within a porous medium (alumina ceramic), precisely in line with the title and objectives. By employing the Darcy-Forchheimer-Brinkman model and utilizing water as the base fluid with single-walled carbon nanotubes (SWCNTs) as nanoparticles, the impact of various parameters such as the magnetic field, nanoparticle concentration, and Darcy number on heat transfer rate are analyzed. Local non-similarity method with the bvp4c solver is used to achieve the solution of the governing equations. The findings indicate that the Darcy number plays the most critical role in enhancing heat transfer, while the magnetic parameter and nanoparticle concentration show less pronounced effects. This conclusion is directly aligned with the study's focus on optimizing the heat transfer process in nanofluid systems, confirming that low magnetic parameter and nanoparticle concentrations, combined with high Darcy numbers, yield optimal results. This contributes to the optimization of nanofluid flows in porous media, with direct implications for improving heat transfer systems in engineering applications such as cooling systems, insulation, and other fluid flow technologies. This dual approach allows for deeper insights into how physical parameters interact, making this research distinct from previous work on nanofluid flow over stretchable surfaces. These results contribute to the ongoing research in nanofluid dynamics and provide a deeper understanding of the interactions within a porous medium. Future studies can expand on this by exploring additional physical parameters to further optimize nanofluid flow systems.

Acknowledgements

We appreciate the support from Universiti Teknikal Malaysia Melaka.

We thank the anonymous referees for their comments and feedback on earlier version of this document.

References

[1] M. Hussain and M. Sheremet, Convection analysis of the radiative nanofluid flow through porous media over a stretching surface with inclined magnetic field, Int. Comm. Heat Mass Transf. 140 (2023), 106559.

[2] N. S. Khashi'ie, N. M. Arifin, M. M. Rashidi, E. H. Hafidzuddin and N. Wahi, Magnetohydrodynamics (MHD) stagnation point flow past a shrinking/stretching surface with double stratification effect in a porous medium, Journal of Thermal Analysis and Calorimetry 139 (2020), 3635-3648.

[3] S. Alao, S. O. Salawu, R. A. Oderinu, A. A. Oyewumi and E. I. Akinola, Viscous heating and thermal gyration of magneto-micropolar fluid particles through an isothermal porous fixed channel with internal non-uniform heat generation: An analytical investigation, Results in Engineering 23 (2024), 102474.

[4] S. Alao, S. O. Salawu, R. A. Oderinu, A. A. Oyewumi, A. A. Yahaya, A. T. Adeosun and A. D. Ohaegbue, Mixed convective and viscous heating effect of electromagnetic Tiwari-Das nanofluid model with permeable wall conditions, Partial Differential Equations in Applied Mathematics (2025), 101181.

[5] S. Alao, S. O. Salawu, R. A. Oderinu, E. I. Akinola, A. A. Oyewumi, A. A. Yahaya and K. A. Salaudeen, Numerical computation of thermal radiation and mixed convective effect on electromagetized Tiwari-Das nanofluid (and) model in a porous microchannel, International Journal of Applied and Computational Mathematics 11(3) (2025), 113.

[6] S. Alao, R. A. Oderinu, B. A. Sanusi, T. A. Oyeyinka and F. J. Ayanbukola, Computational investigation of magnetohydrodynamics Casson Micropolar fluid flowing past a permeable linearly stretchy wall with heat source, Journal of the Nigerian Society of Physical Sciences (2025), 2577.

[7] R. A. Oderinu, F. J. Ayanbukola, S. Alao, B. A. Sanusi and T. A. Oyeyinka, Mixed convective and nonuniform internal heat generation effect on hydromagnetic micropolar fluid flowing across a permeable stretchy wall: A numerical investigation, Heat Transfer 54(3) (2025), 1940-1951.

[8] R. A. Oderinu, T. A. Oyeyinka, S. Alao, F. J. Ayanbukola and B. A. Sanusi, Mixed convection and permeability effects on magnetohydrodynamic Williamson fluid flow over an inclined stretchy surface with radiation influence: Analytical Investigation, Engineering Reports 7(4) (2025), e70078.

[9] N. S. Khashi'ie, M. F. Mukhtar, N. A. Zainal, K. Hamzah, I. Waini, A. R. Kasim and I. Pop, Sensitivity analysis of MHD hybrid nanofluid flow over a radially shrinking disk with heat generation, J. Adv. Res. Fluid Mech. Therm. Sci. 117(2) (2024), 116-130.

[10] K. Venkatadri, H. F. Öztop, V. R. Prasad, S. Parthiban and A. O. Bég, RSM-based sensitivity analysis of hybrid nanofluid in an enclosure filled with non-Darcy porous medium by using LBM method, Numer. Heat Transf. A. 85(6) (2024), 875-899.

[11] S. Panda, S. Ontela, S. R. Mishra and P. K. Pattnaik, Response surface methodology and sensitive analysis for optimizing heat transfer rate on the 3D hybrid nanofluid flow through permeable stretching surface, J. Therm. Anal. Calorim. 148(14) (2023), 7369-7382.

[12] S. Rashidi, M. Bovand and J. A. Esfahani, Structural optimization of nanofluid flow around an equilateral triangular obstacle, Energy 88 (2015), 385-398.

[13] F. Ren, Q. Li, P. Wang and L. Xin, Multi-objective optimization of nanofluid thermal performance in battery cold plates using computational fluid dynamics, Applied Thermal Engineering 260 (2025), 125034.

[14] S. Muhammad, D. Hussain and M. A. Abbas, Optimization of entropy generation on peristaltic flow of nanofluid having compliant walls by RSM: Sensitivity analysis, International Journal of Thermofluids 23 (2024), 100811.